Brief Communication

MOLECULAR METABOLISM

Pre-clinical cancer cachexia causes glucose hypermetabolism prior to overt weight loss

Emma Frank[1], Kaspar W. Persson[2], Pauline Morigny[3,4,5], Zakarias Kefil Jensen Ogueboule[1], Tang Cam Phung Pham[1,6], Jonas R. Knudsen[2], Maria Rohm[3,4,5], Lykke Sylow[1,*], Steffen H. Raun[1,]**

ABSTRACT

Purpose: Cancer cachexia is a life-threatening complication of advanced malignancies, driven by profound systemic metabolic reprogramming and anorexia. Insulin action is markedly impaired in patients with cancer and may contribute directly to cachexia pathogenesis. However, the interplay between weight loss, food intake, and cancer-associated metabolic rewiring in cachexia remains poorly defined. Clarifying this relationship is essential for identifying the fundamental drivers of cachexia and for developing effective therapeutic strategies.

Methods: We assessed metabolic rewiring by temporal evaluation of glucose tolerance and isotopic tracers to determine muscle insulin-stimulated glucose uptake in male cachectic and non-cachectic C26- and KPC-tumor-bearing, as well as healthy mice undergoing food restriction.

Results: Cachectic C26- and KPC-tumor mice showed increased glucose tolerance compared to non-tumor-bearing control mice, and non-cachectic tumor-bearing mice. Increased glucose tolerance appeared prior to overt muscle loss, independent of tumor size and changes in food intake. Ex vivo insulin-stimulated glucose uptake was elevated in soleus (+78%) and extensor digitorum longus (+35%) muscle from cachectic C26-tumor mice with anorexia compared to weight stable C26-tumor mice and control mice. This increase was associated with enhanced AKT signaling. Food restriction in healthy mice increased glucose tolerance, insulin-stimulated glucose uptake *ex vivo*, and AKT signaling.

Conclusions: Our findings suggest that glucose hypermetabolism appears prior to overt weight loss in pre-clinical cachexia, whereas late-stage cachexia with anorexia increased skeletal muscle insulin responsiveness. This highlights AKT signaling as a key node connecting nutrient status with muscle metabolism in cancer cachexia.

Keywords Cancer cachexia; Muscle; Insulin sensitivity; Glucose metabolism; Food restriction

1. INTRODUCTION

Cancer cachexia is a multifactorial metabolic syndrome characterized by involuntary loss of skeletal muscle mass, with or without concomitant fat loss, due to reduced appetite and systemic metabolic rewiring. Affecting up to 80% of patients with advanced cancer, cachexia contributes substantially to morbidity, treatment intolerance, mortality, and impairs quality of life [1,2]. Systemic metabolic rewiring in cancer involves reduced insulin responsiveness in skeletal muscle [3,4], possibly contributing to the pathogenesis of cachexia. However, the interplay between weight loss, reduced food intake and cachexia-associated metabolic reprogramming remains poorly defined. Yet, it is central in delineating the mechanisms that drive cachexia and in identifying treatment targets.

Skeletal muscle, being a major site of glucose disposal under insulin-stimulated conditions, is likely to play a central role in the metabolic disturbances associated with cancer. Clinically, cancer is often associated with systemic insulin resistance and impaired glucose tolerance in patients [4–6] similarly to the insulin resistance observed in patients with type 2 diabetes [7]. Accordingly, patients with cancer have a higher risk of developing type 2 diabetes after their diagnosis [8,9]. In the preclinical setting, weight-stable LLC-tumor-bearing mice display impaired insulin tolerance and skeletal muscle insulin resistance [10–12]. Because insulin is an anabolic hormone, insulin resistance might contribute to cancer cachexia. This has been indicated by some preclinical evidence showing that insulin resistance precedes cachexia and that cachexia can be delayed by insulin sensitizers in a mouse model of cachexia [13,14]. Moreover, patients with cancer and diabetes display a greater weight loss compared to patients with cancer but without diabetes [15]. Yet, cachectic patients did not exhibit insulin resistance, in contrast to the general cancer patient population [4] and weight stable tumor-bearing mice

[1]The Department of Biomedical Sciences, Faculty of Health and Medical Sciences, University of Copenhagen, Copenhagen, Denmark [2]Department of Nutrition, Exercise and Sports, Faculty of Science, University of Copenhagen, Denmark [3]Institute for Diabetes and Cancer (IDC), Helmholtz Munich, Neuherberg, Germany [4]Joint Heidelberg-IDC Translational Diabetes Program, University Hospital, Heidelberg, Germany [5]German Center for Diabetes Research (DZD), Munich, Germany [6]Institute for Mitochondrial Diseases and Aging, Cologne Excellence Cluster on Cellular Stress Responses in Aging-Associated Diseases (CECAD) and Center for Molecular Medicine (CMMC), Medical Faculty, University of Cologne, Cologne, Germany

*Corresponding author. E-mail: Lykkesylow@sund.ku.dk (L. Sylow).

**Corresponding author. E-mail: steffenraun@sund.ku.dk (S.H. Raun).

Received March 16, 2026 • Revision received June 26, 2026 • Accepted July 13, 2026 • Available online 17 July 2026

https://doi.org/10.1016/j.molmet.2026.102422

[10,11,16], as indicated by a recent systematic review and meta-analysis [17]. Moreover, at basal conditions, muscle from multiple cachectic mouse models was recently shown to develop glucose hypermetabolism [18]. Thus, it remains unclear whether cachexia is associated with altered insulin responsiveness, and potential mechanisms linking cancer cachexia with insulin action are unresolved.

A key contributor to cachexia that could influence insulin action is the reduced food intake associated with cancer cachexia. Anorexia in patients and tumor-bearing mice exacerbates weight loss by limiting energy and nutrient availability, accelerating muscle and fat wasting, but it is not the sole driver of cachexia [19–21]. However, reduced caloric intake itself can significantly affect glucose metabolism [22–24], which could be a potential confounding factor in interpreting metabolic outcomes in pre-clinical cancer cachexia models and in the clinic.

In this study, we aimed to investigate whole-body and skeletal muscle-specific glucose metabolism across several models of pre-clinical cancer cachexia and how short-term decreased food intake may be a confounding factor in the interpretation of the metabolic effects of cachexia.

2. METHODS

2.1. Animal experiments

Cohort 1, 3 & 4: All experiments were approved by the Danish Animal Experimental Inspectorate (License: 2021-15-0201-01104 and 2021-15-0201-01085). Mice were maintained under a 12:12 h light/dark photocycle at ambient (22 ± 1 °C) temperature with nesting material. All mice received a rodent chow diet (Altromin #1324; Chr. Pedersen, Denmark) and water ad libitum. Male mice were group-housed for cancer studies, and single-housed for the food-restriction study. Cohort 2: Animal experiments were conducted in 9 week-old male Balb/c mice (Charles River Laboratories Germany). Animals were housed under specific pathogen-free conditions on a 12 h light/dark cycle at 22 °C and had unlimited access to food (chow diet Altromin #1314) and water. Animal handling and experimentation were performed according to the institutional animal welfare officer and license from the state ethics committee and government of Upper Bavaria (ROB-55.2-2532. Vet_02-18-93).

2.2. Tumor-bearing mouse models

Cohort 1, 3 & 4: 12-week-old male Balbc/J mice (Janvier, Denmark) were used for Colon26-cancer (C26) studies, and 14-week-old male C57BL/6JBomTac (Taconic, Denmark) were used for KPC studies. All mice were group-housed in pairs and randomly assigned to either the cancer or control group. C26 adenocarcinoma cells (kind gift from Dr. Adam Rose) were maintained at 37 °C, 5% CO2, in RPMI 1640 medium (Gibco, #11875093) supplemented with 10 % fetal bovine serum (FBS, Gibco #F0804) and 1% antibiotic-antimycotic (ThermoFisher, #15140122). KPC cells (CancerTools, #153474) were maintained at 37 °C, 5% CO_2, in DMEM (Gibco, #11965092) supplemented with 10 % FBS (Gibco #F0804) and 1% antibiotic-antimycotic (ThermoFisher, #15140122). All mice were shaved on the right flank the day before cancer inoculation. On the day of inoculation, C26 or KPC cells were trypsinized and washed twice with PBS (centrifuged for 3 min at 1,600 g), followed by resuspension in PBS. Next, all mice were injected subcutaneously into the flank with PBS with or without C26 or KPC cells for a final concentration of 5×10^5 cells or 1×10^6, respectively. Mice were terminated when reaching humane endpoints following the tumor guidelines from the Danish Animal Experimental Inspectorate (tumors >14 mm - average length and width or ulcerations >5 mm). C26-cancer mice were divided into non-cachexia (tumor with no weight loss) or cachexia (tumor with weight loss) groups. Cohort 2: Animals were injected with 1 million NC26 (non-cachectic mouse colon carcinoma) or C26 cells (mouse colon carcinoma) or a similar amount of PBS (Thermo Fisher Scientific #14190250), subcutaneously in the flank. Mice were monitored for 2–4 weeks and tumor growth, body weight and Body Condition Score (BCS) were evaluated daily. Mice were sacrificed by an overdose of ketamine-xylazine the day after the last assay (body weight loss >10 %) or before if they reached humane endpoint (tumor ulceration).

2.3. Food restriction, pair-fed to cachectic C26 tumor-bearing mice

12-week-old male Balbc/J mice (Janvier, Denmark) were used for the pair-feeding study. All mice were single-housed, and food intake was recorded daily during the last week of the experiment. The last three days, the food intake was reduced by approximately 30%, corresponding to what was observed in cachectic C26-cancer mice.

2.4. Body composition

Cohort 1, 3 & 4: Body mass composition was assessed by nuclear magnetic resonance using an EchoMRI™ (USA) or a Bruker LF90II Body Composition Analyser (Bruker) for total body, lean, and fat mass. All mice were MRI scanned before cancer cell inoculation and the day before termination. The tumor mass from dissections was subtracted from the total body weight and lean mass. Cohort 2: Body composition was evaluated by EchoMRI™ (USA).

2.5. Grip strength

Grip strength was assessed in the week before termination. Grip strength assessment was performed using a grip meter (Bioseb). The mice were held by the base of the tail and briefly left to hover over the grid and allowed to grab with all four paws. Once grabbed, the mice were gently pulled back in a horizontal position. This was repeated three times for each mouse, and the maximal recording was used as final force readout.

2.6. Glucose tolerance test

Cohort 1, 3 & 4: All mice were fasted for 4 h before the glucose tolerance test (GTT). D-mono-glucose (2 g kg^{-1} bw) was administered via intraperitoneal injections, and blood was collected from the tail vein. Blood glucose levels were determined at timepoints 0, 20, 40, 60, 90, and 120 min using a glucometer (Bayer Contour, Bayer, Switzerland). Blood aliquots from timepoints 0 and 20 min were centrifuged at 13,000 rpm for 5 min at 4 ° C, and plasma was collected and frozen in liquid nitrogen. Insulin levels were measured using the Mouse Ultrasensitive Insulin ELISA (#80-INSMSU-E01ALPCO Diagnostics, USA). Cohort 2: Glucose tolerance tests were performed one and two weeks after cancer cell injection, and once animals started to develop cachexia (body weight loss between 5 and 10%). Animals were fasted for 6 h before receiving a dose of 2 g kg^{-1} bw of glucose intraperitoneally. Glycemia was recorded via a micro-puncture of the tail vein, using a glucometer (Accu-Check #Performa).

2.7. *Ex vivo* insulin-stimulated glucose uptake

Soleus and extensor digitorum longus (EDL) muscles were rapidly isolated from anesthetized mice, and non-absorbable 4–0 silk suture loops (Look SP116, Surgical Specialties Corporation) were attached at both ends as previously described [11]. In brief, the muscles were placed in a DMT Myograph system (820MS; Danish Myo Technology, Hinnerup, Denmark) and incubated at resting tension (4–5 mN at

30 °C) in oxygenated (95% O_2, 5% CO_2) Krebs—Ringer buffer. Isolated muscles were pre-incubated in Krebs—Ringer buffer for 5 min, followed by 20 min of either control (vehicle) or maximal insulin stimulation (60 nM). During the last 10 min, 0.75 μCi/mL [3H]-2DG and 0.225 μCi/mL [14C]-Mannitol were added (including insulin). Following the insulin stimulation, muscles were immediately rinsed in ice-cold saline and snap-frozen. Muscle-specific 2DG-uptake was measured on tissue lysates [25].

2.8. Lysate preparation and immunoblotting

Muscle tissues were homogenized in a modified GSK3-buffer and prepared for immunoblotting as previously described in detail [16]. Coomassie stains were used as control for loading, as this provides a better loading control compared to other known proteins referred to as housing genes [26,27]. The catalog number for all antibodies are described in the legend for Fig. 4.

2.9. Statistical analysis

Data are presented as mean ± SEM and individual data points (when applicable) and analyzed using GraphPad Prism 10. Statistical tests were performed using paired/non-paired *t*-tests or repeated/no-repeated two-way analysis of variance (ANOVA) as applicable. Multiple-repeated two-way ANOVAs were performed in analyses, including all experimental groups testing for the effect of C26, KPC, or food restriction. Sidak's post hoc test was performed when ANOVA revealed significant main effects and interactions. The significance level was set at $\alpha = 0.05$.

3. RESULTS

3.1. C26-cachectic mice exhibit improved glucose tolerance and elevated skeletal muscle insulin-responsiveness *ex vivo*

We first determined classical manifestations of cachexia in the C26-cancer model to establish the effects of cachexia on glucose metabolism. During tumor-progression, the mice underwent a GTT at day 14, measurement of food intake at day16—18, MRI-scan and grip strength at day 18, before being terminated where *ex vivo* insulin-stimulated glucose uptake was measured (experimental setup is depicted in Fig. 1A). C26 mice lost body weight during the experiment with a difference on day 18 in comparison to control mice (Fig. 1B). At day 14, prior to separation based on weight loss, C26 tumor-bearing mice showed similar fasting plasma glucose levels (Fig. 1C) and an increased glucose tolerance compared to control mice (Fig. 1D), contrasting previous findings [10,28]. Glucose excursions during the GTT were inversely correlated with tumor volume, potentially reflecting cachexia-associated metabolic remodeling or tumor glucose sequestration (Fig. 1E). The observed changes in glucose tolerance were independent of glucose-stimulated plasma insulin (Fig. 1F).

At termination, the tumor-bearing C26 mice were separated into weight-stable (n = 6, <10% weight loss) and cachectic mice (n = 9, >10% weight loss). Here, after termination the cachectic mice had a 20% reduction in body mass 20 days after inoculation, while weight stable mice maintained their body mass having <10% weight loss with no statistical significance. Control mice had a minor body mass gain of 5% (Fig. 1G). Average tumor size was approximately 80% larger in cachectic mice compared to weight stable mice (Fig. 1G). Similarly, cachectic mice displayed a 15% reduction in lean body mass, whereas both weight stable and control mice maintained lean body mass (Fig. 1H). Cachectic mice exhibited a 75% reduction in fat mass, while weight stable (p = 0.0510) and control mice exhibited a ~20% increase in fat mass (Fig. 1I).

At termination, we weighed selected muscles and adipose tissues. Only cachectic mice had lower weights for gastrocnemius (Gast, −17%), tibialis anterior (T. anterior, −18%), and perigonadal adipose tissue (pWAT, −95%) compared to control mice. Heart tissue weights were reduced in both tumor-bearing groups by 8% and 14% for weight stable and cachectic mice, respectively. Brown adipose tissue (BAT) was 17% and 47% lower for weight stable and cachectic mice, respectively, compared to control mice. The spleen was similarly increased in both tumor-bearing groups by approximately 100% (Fig. 1J), indicative of similar systemic inflammatory burden despite marked differences in tumor mass and cachectic phenotype. Despite no significant reduction in muscle weights, we detected a 17% reduction in grip strength in weight stable mice, while cachectic mice showed a reduction of 27% compared to control mice (Fig. 1K). Food intake was assessed three days prior to termination and a reduction (~40% vs. controls) was observed exclusively in cachectic mice (Fig. 1L).

Since skeletal muscle is the primary site for glucose disposal, we proceeded to determine insulin-stimulated glucose uptake in soleus and EDL *ex vivo* of C26 weight-stable and cachectic mice. In the soleus muscles, insulin led to increased glucose uptake in all groups (Fig. 1M). However, cachectic mice showed ~80% higher response to insulin compared to weight stable tumor-bearing mice and control mice (Fig. 1M). Similarly, in the EDL muscle, cachectic mice showed a 35—40% elevation in insulin response compared to weight stable and control mice (Fig. 4N). Importantly, the elevation of insulin-stimulated glucose uptake in EDL muscle of cachectic mice was also affected by a slight elevation of the basal glucose uptake as well (Fig. 4N). Thus, cachexia was associated with elevated insulin responsiveness towards glucose uptake in mouse muscle.

Together, our results demonstrate that C26 tumor-bearing mice develop increased glucose tolerance and muscle insulin-stimulated glucose uptake concurrently with muscle and fat mass loss that end-stage cachexia in the C26 mouse model is associated with reduced food intake.

3.2. Increased glucose tolerance appears prior to overt weight loss and independent of tumor-size in C26 tumor-bearing mice

As the glucose tolerance in the C26 tumor-bearing mice was correlated to tumor size, we next wanted to investigate the temporal development of altered glucose tolerance in both a cachectic C26 tumor model, and a C26 mouse model that does not develop cachexia (non-cachectic C26, NC26). Here, the mice were subjected to a glucose tolerance test and an MRI on day 7, 14 and as soon as they developed cachexia (16—18 days after the inoculation of cancer cells (cohort 2, Fig. 2A). Body mass (Fig. 2C), lean body mass (Fig. 2D), and fat mass (Fig. 2E), were maintained from day 0 to day 7. From day 7—14, the cachectic C26 mice lost a modest amount of body mass (Fig. 2C), primarily owing to a loss of fat mass (Fig. 2E), not lean mass (Fig. 2D). At the end of the intervention, the cachectic C26 mice had lost a significant amount of both lean (Fig. 2D) and fat mass (Fig. 2E), leading to overall reduced body mass (Fig. 2C). Both the non-cachectic C26 and the control mice had increased body mass and lean mass at the end of the intervention, with no change in fat mass (Figure 2C—E). Thus, we were here able to investigate the temporal response on glucose metabolism in pre-clinical cachexia without the confounder of changes in tumor size.

First, fasting plasma glucose decreased in the cachectic C26 mice at the end of the intervention compared to day 7, where this was not observed within the two other groups of mice (Fig. 2F). At day 7, the cachectic mice showed comparable glucose tolerance relative to the

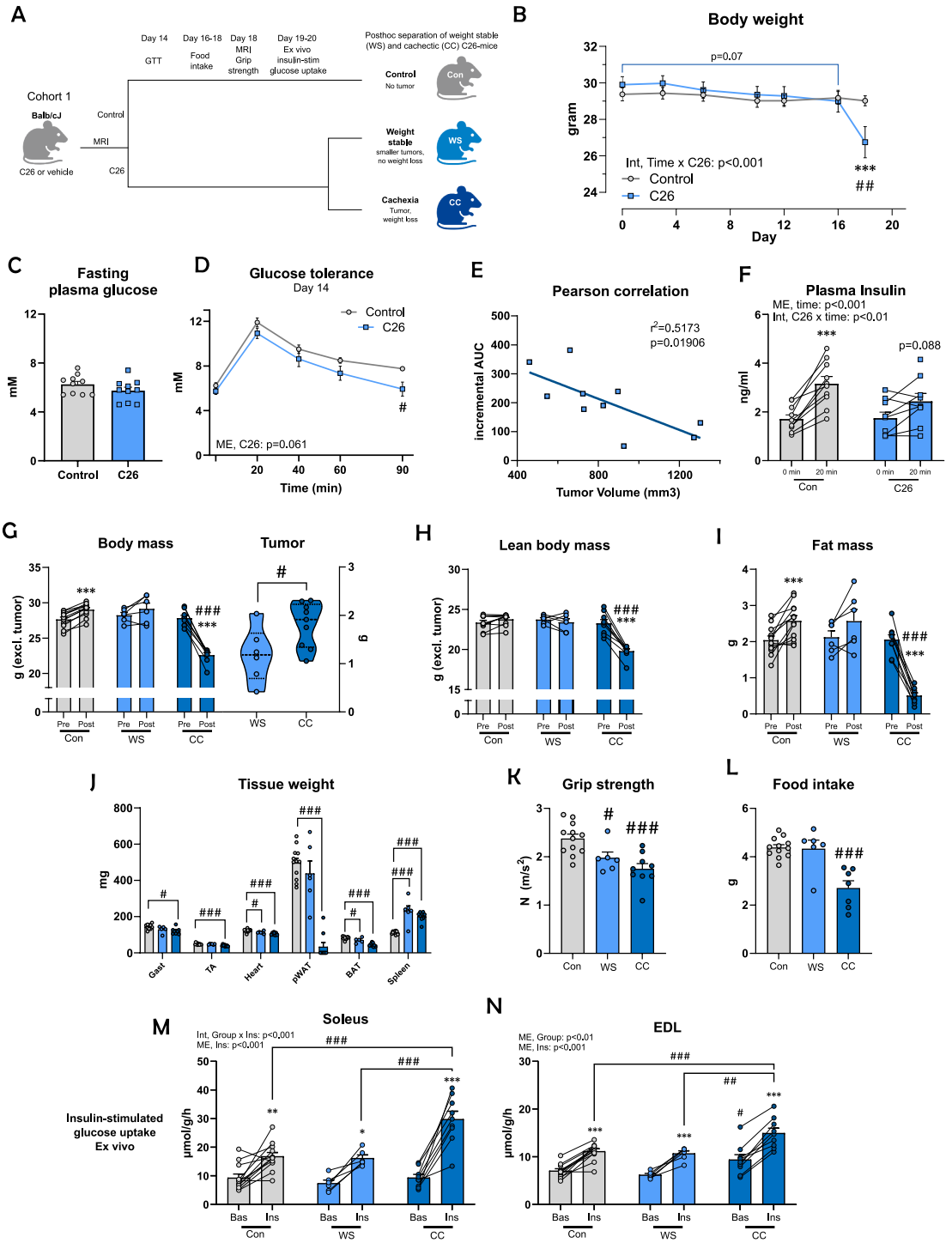

Figure 1: C26 tumor-bearing mice exhibit improved glucose tolerance despite lowered muscle and fat mass.
A) Study design of the C26-cancer study (cohort 1). **B)** Body weight during the intervention. **C)** Fasting plasma glucose. **D)** Glucose tolerance test on day 14 after inoculation. **E)** Pearson correlation analysis of tumor size and incremental area under the curve. **F)** Plasma insulin levels from time-point 0 and 20 min during the glucose tolerance test. Of not, the sample number is lower due to lack of plasma collected during the tolerance test. **G)** Body mass and tumor weight, **H)** Magnetic Resonance Imaging-derived lean body mass. **I)** Magnetic Resonance Imaging-derived fat mass. **J)** Tissue weights at termination from gastrocnemius (Gast), tibialis anterior (TA), heart, perigonadal white adipose tissue (pWAT), brown adipose tissue (BAT), and spleen. **K)** Grip strength measured on day 16–18 before termination. **L)** Food intake the last three days before termination. **M)** *Ex vivo* insulin-stimulated (60 nM) glucose uptake in the soleus muscle. **N)** *Ex vivo* insulin-stimulated (60 nM) glucose uptake in the EDL muscle. Abbreviation: C26 = Colon26, Con = control, WS = weight stable, CC = cancer cachexia, Int = interaction, ME = main effect, AUC = area under the curve. Values are shown as mean ± SEM, including individual values, and as mean ± SD when individual values are not shown. Effect of C26: # = $p < 0.05$, ## = $p < 0.01$, ### = $p < 0.001$. Effect of time: * = $p < 0.05$, ** = $p < 0.01$, *** = $p < 0.001$.

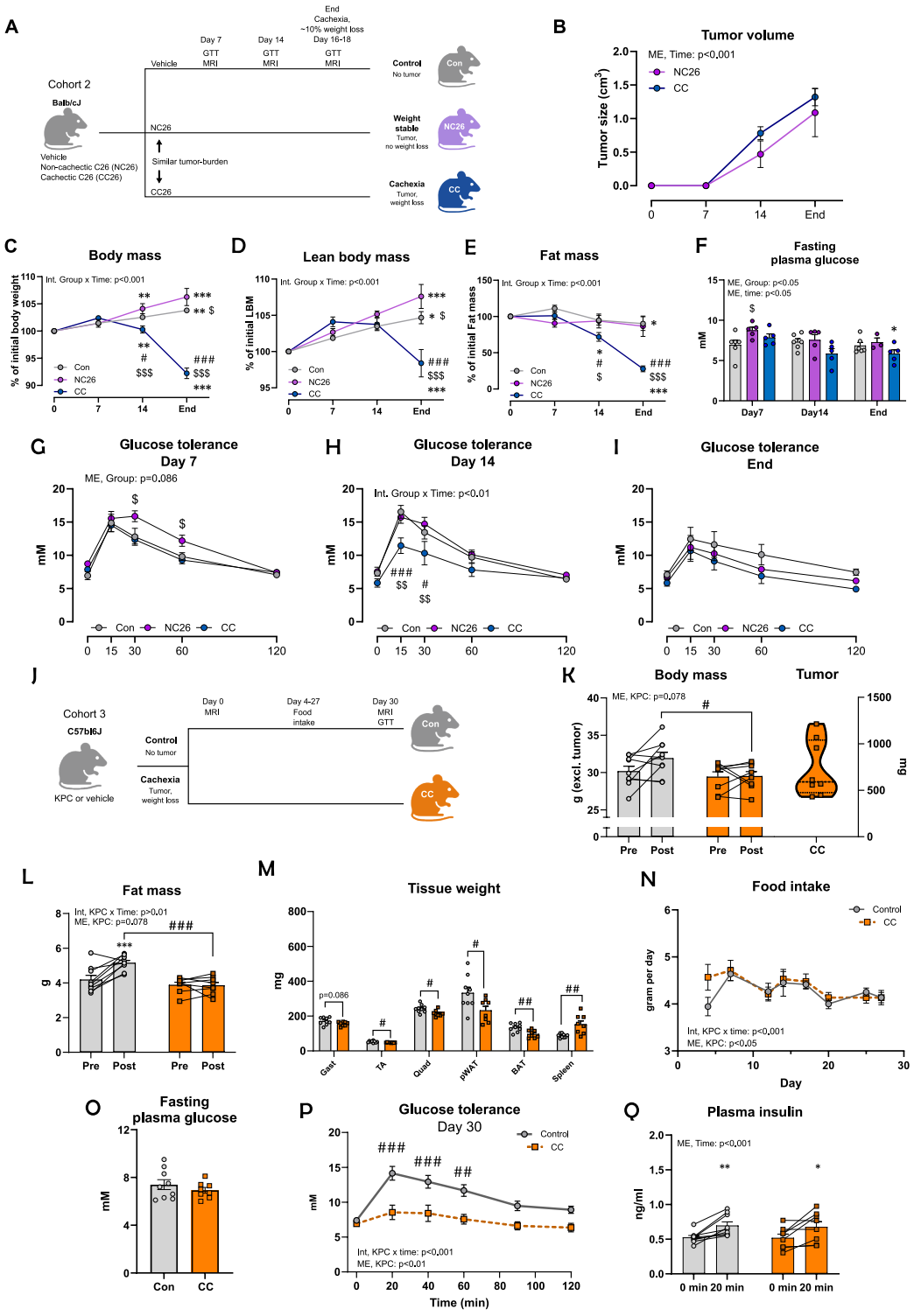

Figure 2: C26 tumor-bearing mice display increased glucose tolerance prior to overt loss of body mass independent of tumor size.
A) Study design of temporal glucose tolerance C26 study (study 2). **B)** tumor volume during the intervention. **C)** Body mass, **D)** Lean body mass, **E)** Fat mass and **F)** fasting plasma glucose during the intervention. Glucose tolerance at **G)** day 7, **H)** day 14, and **I)** at termination of the study. **J)** Study design of cohort 3, the KPC-cancer study. **K)** Body mass and tumor mass. **L)** Magnetic Resonance Imaging-derived fat mass. **M)** Tissue weights at termination from Gast, TA, quadriceps (Quad), pWAT, BAT, and spleen. **N)** Food intake during the intervention. **O)** Fasting plasma glucose. **P)** Glucose tolerance test on day 30 after inoculation. **Q)** Plasma insulin levels from time-point 0 and 20 min during the glucose tolerance test. Abbreviation: C26 = Colon26, Con = control, NC26 = Non-cachectic C26, CC = cancer cachexia, Int = interaction, ME = main effect. Values are shown as mean ± SEM, including individual values. Effect of C26 or KPC: # = $p < 0.05$, ## = $p < 0.01$, ### = $p < 0.001$. Effect of time: * = $p < 0.05$, ** = $p < 0.01$, *** = $p < 0.001$. Effect of NC26: $ = $p < 0.05$, $$ = $p < 0.01$, $$$ = $p < 0.001$.

control mice, where the non-cachectic C26 mice showed a slight dimished glucose tolerance compared to the cachectic mice (Fig. 2G). At day 14, the cachectic mice showed increased glucose tolerance compared to both control and non-cachectic C26 mice (Fig. 2H), similar to what was observed in cohort 1. At the termination of the experiment, the glucose tolerance showed similar trend while not being statistically significant (Fig. 2I). Importantly, we did observe a day-to-day variance in our control mice, which is a limitation of the experimental setup. Thus, this variability may affect the ability to observe the full effect of cachexia on glucose tolerance in our mice. Collectively, these data show that C26 mice develop increased glucose tolerance reflecting a temporary metabolic adaptation which appears prior to overt weight/lean mass loss.

3.3. The cachectic KPC tumor-bearing mice also display markedly elevated glucose tolerance

Having observed elevated glucose tolerance in the cachectic C26 model, we next assessed glucose tolerance in another pre-clinical cachexia model, the KPC model (cohort 3, Fig. 1J). KPC tumor-bearing mice had an 8% lower body mass at termination (Day 31) compared to control mice, indicative of cachexia (Fig. 1K). Similarly, fat mass was 25% lower in cachectic mice at termination compared to control mice (Fig. 1L). Measurements of tissues at termination revealed that cachectic KPC mice had lower muscle and adipose tissue weight compared to control mice (Gast −10% p = 0.081, T. anterior −9%, quadriceps −11%, pWAT −30%, BAT -28%), while the spleen weight was increased by 75% in cachectic mice (Fig. 1M). Importantly, these changes were observed without any changes in food intake of the KPC mice (Fig. 2N). On day 30, fasting plasma glucose was not altered in KPC mice (Fig. 2O). However, similar to the observation in C26 tumor-bearing mice, and in line with previous literature of the KPC model [29], KPC tumor-bearing mice had a marked improvement in glucose tolerance (Fig. 1P). The change in glucose tolerance was independent of glucose-stimulated plasma insulin (Fig. 1Q). Thus, pre-clinical cachexia leads to increased glucose tolerance prior to overt weight/lean mass loss and independent of changes in food intake.

3.4. Three days of food restriction lowers body weight, muscle mass, and fat mass in mice

Anorexia is a key contributor to the manifestations of cachexia, as also observed in our cachectic C26 mice at a late-stage of the intervention (Fig 1), and lowered food intake is known to impact metabolism [22–24]. While likely not contributing to the initial change in glucose metabolism of cachectic mice, decreased food intake may affect the glucometabolic phenotype observed in late-stage cachexia. We therefore executed a 3-day food restriction study (−30%, mimicking the reduced food intake in late-stage C26 cachectic mice, Fig 1) in non-tumor bearing male mice to assess whether reduced food intake could explain the improved insulin responsiveness observed in cachectic mice (Fig. 3A). First, we measured body weight daily and discovered that food-restricted mice lost 1.2 g (−3.9%) body weight on average after 3 days, compared to control mice who gained 0.7 g (2.1%) body weight (Fig. 3B). We measured tissue weights and observed a reduction in tissue weights of all skeletal muscles and adipose tissues upon food restriction (TA -4%, Gast −7%, Quad −7%, iWAT −34%, pWAT −22%, BAT -23%, spleen −16%), while the heart weight was similar (Fig. 3C). Despite lower muscle

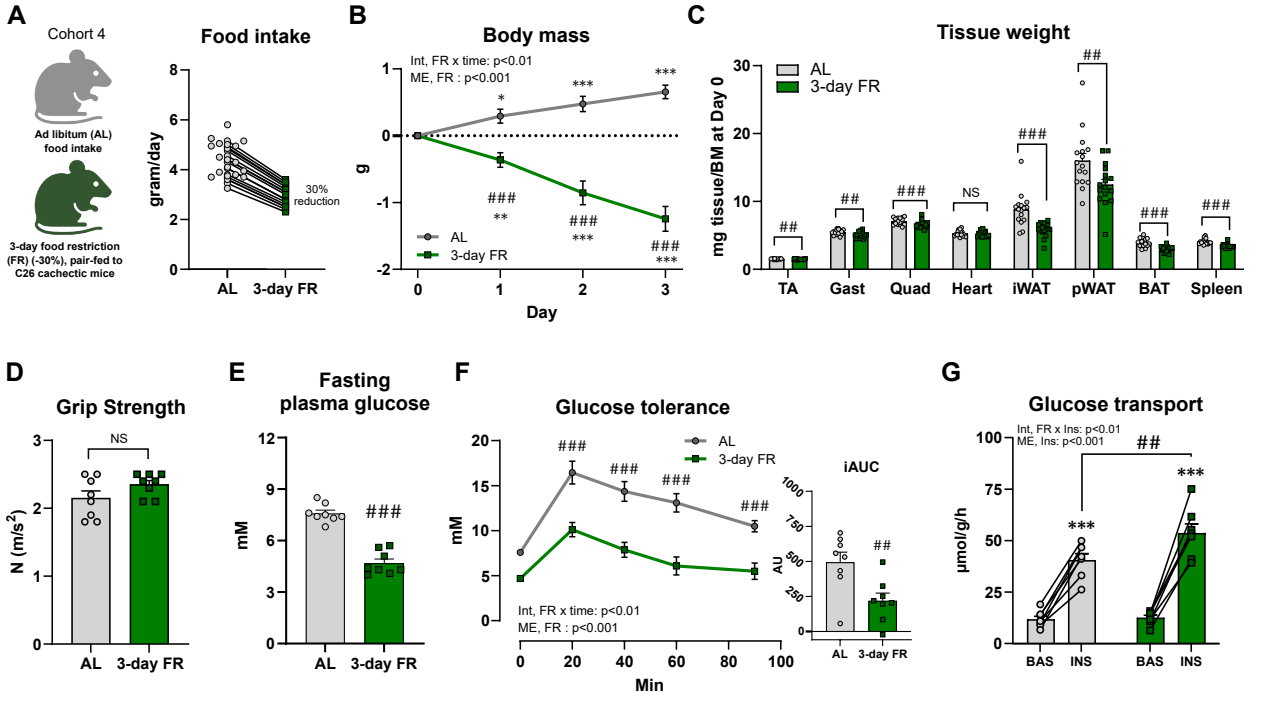

Figure 3: Three days of food restriction in mice improves glucose tolerance, *but does not alter grip strength in lean mice*.
A) Study design of the food restriction study. **B)** Body weight measured during the food restriction period. **C)** Tissue weights at termination from TA, Gast, Quad, heart, inguinal white adipose tissue (iWAT), pWAT, BAT, and spleen. **D)** Grip strength measured after 3 days of food restriction. **E)** Fasting plasma glucose. **F)** Glucose tolerance test and incremental area under the curve (iAUC) after three days of food restriction. **G)** *Ex vivo* insulin-stimulated (60 nM) glucose uptake in the soleus muscle. Values are shown as mean ± SEM, including individual values, and as mean ± SD when individual values are not shown. Effect of 3-days food restriction: * = $p < 0.05$, ** = $p < 0.01$, *** = $p < 0.001$.

weights in food-restricted mice, grip strength was unaffected (Fig. 3D), indicating that anorexia may underlie some body weight loss but does not compromise muscle function in tumor-bearing mice.

To investigate if anorexia may underline some of the improvements in glucose tolerance, we next determined the glucose tolerance in 3-day food-restricted Balb/c mice. Importantly, food-restriction led to a marked reduction in fasting plasma glucose (Fig. 3E). Interestingly, food-restriction markedly improved glucose tolerance with a 56% reduction in incremental AUC (taking the lower fasting plasma glucose into account) compared to ad libitum fed control mice (Fig. 3F). We then proceeded to determine *ex vivo* insulin-stimulated glucose uptake in the soleus muscles. We were intrigued to see that food-restricted mice had a higher insulin response (30%) compared to control mice (Fig. 4G). Collectively, reduced food intake in a healthy mouse led to modest weight loss, increased glucose tolerance and elevated muscle insulin responsiveness, but did not affect physical function.

3.5. Elevated Akt signaling coincides with higher insulin-stimulated glucose uptake in C26 cachectic mice

After demonstrating an evidently higher muscle insulin responsiveness in cachectic mice (cohort 1), we proceeded to investigate intramyocellular insulin signaling. We found a reduction in protein contents of Glucose transporter 4 (GLUT4) (−20%), Glycogen Synthase (−13%, $p = 0.057$), Akt2 (−22%, $p = 0.057$), p70S6K (−17%), and rS6 (−29%, $p = 0.068$) in C26 cachectic compared to control mouse soleus muscle (Fig. 4A). In contrast, Hexokinase II, Pyruvate Dehydrogenase, TBC1D4, GSK3β, and PRAS40 were unaffected (Fig. 4A). It is well known that insulin acts as an anabolic hormone to activate the Akt signaling pathway stimulating glucose uptake and glycogen synthesis in skeletal muscle [30]. Thus, we investigated Akt phosphorylation and downstream targets in response to insulin. In control and C26 weight stable mice, we observed a 2-fold and 2.5-fold increase in phosphorylated (p) AKT^{thr308}, respectively, in the insulin-stimulated soleus muscle. Yet, in cachectic mice, there was an even higher 4.4-fold increase by insulin compared to the non-stimulated muscle (Fig. 4B). Correspondingly, $pAKT^{ser473}$ increased by 3.8-fold upon insulin stimulation in control and weight stable mice, while cachectic mice exhibited a remarkable 8.5-fold increase (Fig. 4C). Yet we observed a similar increase (3.3- and 3.9-fold) in $pTBC1D4^{thr642}$, a downstream target of AKT, in insulin-stimulated soleus muscle from weight stable and cachectic mice, respectively, compared to a 2.4-fold increase in control mice (Fig. 4D). Akt phosphorylates several downstream targets. In the insulin-stimulated soleus muscle from cachectic mice, we found a higher increase in $pGSK^{ser9}$ (3.3-fold, Fig. 4E) and $pGSK^{ser21}$ (2.6-fold, Fig. 4F) compared to control and weight stable mice (2.0- and 1.8-fold, respectively). PRAS40 is a direct downstream target of AKT during insulin stimulation [31,32]. We detected an elevated abundance of $pPRAS40^{thr246}$ in insulin-stimulated cachectic soleus muscles (4.8-fold), compared to both control and weight stable mice (3.3-fold) (Fig. 4G).

Thus, the elevated insulin-responsiveness in cachectic muscle exists despite a reduction of the main glucose transporter (GLUT4), likely circumvented by elevated AKT signaling.

3.6. Reduced food intake elevates AKT signaling

In line with our observations in C26 cachectic mice, AKT signaling was also elevated in food-restricted mice (cohort 4). This was evidenced by, $pAKT^{thr308}$ increasing 8-fold in response to insulin in food-restricted mice compared to 5-fold in control mice (Fig. 4H). Likewise, $pAKT^{ser473}$ increased by 7-fold in response to insulin in food-restricted mice compared to 4-fold in control mice (Fig. 4I). In addition, we found a 6-fold increase by insulin in $pTBC1D4^{thr642}$ in food-restricted mice, which was only increased by 3-fold in control mice (Fig. 4J), while GSK3 and PRAS40 were phosphorylated to a similar extent during insulin stimulation (Fig. 4K-L).

Taken together, our findings show that reduced food intake in the later-stage cachexia can affect the enhanced skeletal muscle insulin responsiveness in late-stage cachectic C26-cancer mice, associated with enhanced Akt signaling.

4. DISCUSSION

In this study, we investigated glucose metabolism and skeletal muscle insulin responsiveness, using three distinct tumor models, C26, NC26 and KPC, and food-restriction in healthy mice. Our results highlight three key discoveries. First, cachexia was associated with increased glucose tolerance in both C26- and KPC tumor-bearing mice, independent of tumor size and food intake. Second, cachectic, but not weight stable, C26 mice exhibit elevated skeletal muscle insulin responsiveness associated with increased Akt signaling. Third, food restriction in healthy mice, mimicking the lower food intake in C26 cachectic mice, caused a similar increase in muscle insulin-responsiveness. These findings suggest that glucose hypermetabolism develops in cachexia prior to overt loss of body/lean mass and independent of changes in food intake, however decreased food intake in late-stage cachexia may contribute to elevated insulin-responsiveness in cachectic muscle.

Our first key finding demonstrates that cachectic C26-tumor-bearing mice exhibited improved glucose tolerance compared to weight stable tumor-bearing mice. Here, we identified a relationship between tumor burden and glucose tolerance, with cachectic highly glucose tolerant mice harboring significantly larger tumors. While it is plausible that larger tumors dispose more glucose during hyperglycemia, contributing to improvements in glucose tolerance, our data from non-cachectic C26 mice with similar tumor-burden suggest otherwise. Our data suggest that there are cachectic factor(s) which lead to glucose hypermetabolism independent of tumor-size and prior to overt weight loss and changes to food intake. A marked metabolic change in glucose utilization is supported by a recent study, using isotopic tracers in C26 cachectic mice, showing that one-carbon metabolism was a tissue-overarching pathway characterized in wasting leading to glucose hypermetabolism [18]. Our second key finding highlights that cancer-associated cachexia is also accompanied by elevated skeletal muscle insulin responsiveness compared to weight stable tumor-bearing mice. This is supported by a recent publication demonstrating that cachectic C26 mice develop increased insulin tolerance compared to control mice [33]. In the soleus and EDL muscles, insulin responsiveness was markedly greater in cachectic compared to both control and weight stable tumor-bearing mice. This was observed despite a reduction in protein content of the key glucose transporter during insulin stimulation, GLUT4 [34]. We [10]and others [14] have previously shown glucose intolerance in tumor-bearing animals. While direct comparisons can be difficult to perform, our data show that timing is essential when investigating glucose metabolism in cachexia. In addition, the data also suggest that the severity of weight loss, with or without anorexia, can affect glucose metabolism. Overall, the current data support the idea of cancer cachexia being associated with elevated glucose tolerance

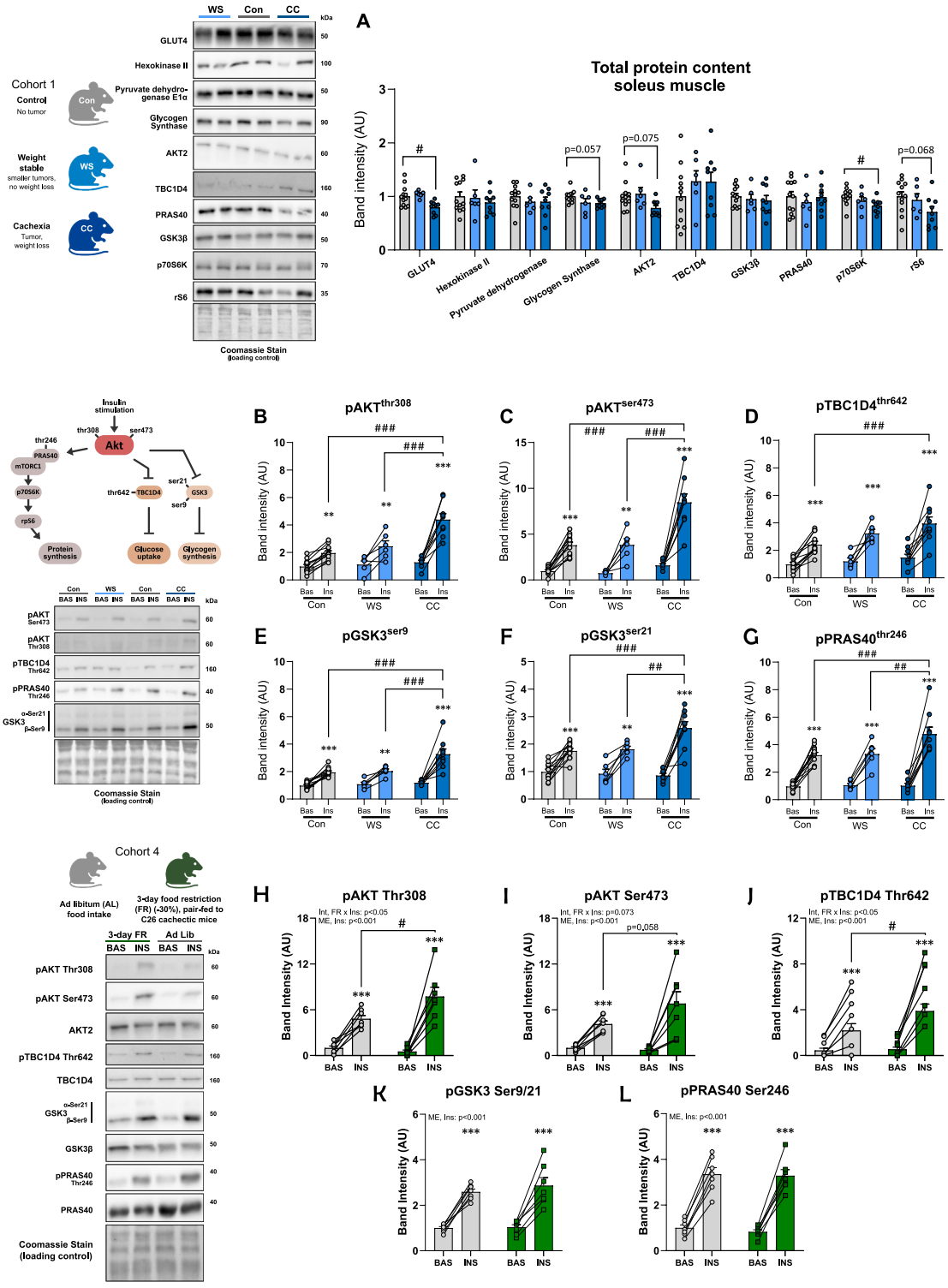

Figure 4: Late-stage cachectic mice and food-restricted healthy mice show increased muscle insulin-responsiveness and elevated Akt signaling.
A) Total protein content in the soleus muscle of GLUT4 (Thermo Fisher Scientific, #PA1-1065), Hexokinase II (Cell Signaling Technology, #2867), Pyruvate dehydrogenase-E1α (D.G. Hardie (University of Dundee, Scotland)), Glycogen synthase (Gift from Prof. Oluf Pedersen), Akt (Cell Signaling Technology, #3063), TBC1D4 (Abcam, ab189890), GSK3β (BD Bioscience, #610202), PRAS40 (Cell Signaling Technology, #2691), p70S6K (Cell Signaling Technology, #2708), rS6 (Cell Signaling Technology, #2217). Protein content is displayed in arbitrary units (AU). Immunoblotting of phosphorylated (p) proteins in the soleus muscle of: **B)** pAKT^{Thr308} (CST, cat#9271), **C)** pAKT^{Ser473} (CST, cat#9271), **D)** pTBC1D4^{thr642} (Cell Signaling Technology, #8881), **E)** pGSK3^{ser9} (Cell Signaling Technology, #9331), **F)** pGSK3^{ser21} (Cell Signaling Technology, #9331), **G)** pPRAS40^{thr246} (Cell Signaling Technology, #2997). **H)** pAKT^{Thr308} (Cell Signaling Technology, cat#9271), **I)** pAKT^{Ser473} (Cell Signaling Technology, cat#9271), **J)** pTBC1D4^{thr642} (Cell Signaling Technology, #8881) **K)** pGSK3$^{ser9/21}$ (Cell Signaling Technology, #9331), **L)** pPRAS40^{thr246} (Cell Signaling Technology, #2997). Representative blots are represented with Coomassie staining as a loading control. Values are shown as mean ± SEM, including individual values. Effect of C26: * = $p < 0.05$, ** = $p < 0.01$, *** = $p < 0.001$.

and insulin responsiveness, although the molecular mechanisms, and whether one-carbon metabolism is involved in this adaptation, remain to be defined.

Our last key finding was that reduced food intake, mimicking food intake in late-stages of cachexia, could contribute to the increased insulin responsiveness in our cachectic mice as a compensatory adaptation to nutrient limitation arising from anorexia and tissue loss. In the late stages of our C26 model, only cachectic mice had significantly reduced food intake with severe lean and fat mass loss. In this context, improved insulin-stimulated glucose uptake in muscle may reflect heightened responsiveness to insulin when exogenous glucose availability is limited, a phenomenon reminiscent of the known effects of caloric restriction [35–37]. Notably, while improved insulin sensitivity may initially represent a compensatory mechanism to preserve energy efficiency, chronic activation of this pathway in the face of catabolic conditions such as cachexia fails to prevent muscle loss. Underscoring this is our finding that cachexia-mimicking food restriction alone did not alter muscle strength measured by grip strength in the current study. Decreased grip strength was observed in both cachectic and weight stable tumor-bearing mice, in line with another study showing decreased muscle function in C26 before cachexia [38]. Accordingly, it is also known that decreased energy intake in cancer is not the sole driver of cachexia [39,40]. Thus, while decreased food intake likely affects the systemic metabolism in the late-stages of cancer cachexia, the pathology of cachexia is complex and involves multiple factors [39].

5. CONCLUSION

In summary, our study reveals that improved glucose tolerance develops prior to overt loss of lean mass, independent of tumor burden and without change in food intake. In the late-stages of cachexia with anorexia, skeletal muscle insulin responsiveness is increased coinciding with enhanced Akt signaling. In healthy mice, food restriction shows similar increased insulin-responsiveness. These findings challenge the assumption that cachexia universally associates with insulin resistance and underscore the need to consider both cancer type, cancer progression, and food intake when interpreting metabolic outcomes in cancer.

CRediT AUTHORSHIP CONTRIBUTION STATEMENT

Emma Frank: Writing – review & editing, Writing – original draft, Visualization, Validation, Resources, Project administration, Methodology, Investigation, Formal analysis, Data curation, Conceptualization. **Kaspar W. Persson:** Writing – review & editing, Writing – original draft, Methodology, Investigation, Formal analysis, Data curation. **Pauline Morigny:** Investigation, Formal analysis, Data curation. **Zakarias Kefil Jensen Ogueboule:** Writing – review & editing, Writing – original draft, Investigation, Formal analysis, Data curation. **Tang Cam Phung Pham:** Writing – review & editing, Writing – original draft, Investigation, Formal analysis, Data curation. **Jonas R. Knudsen:** Writing – review & editing, Writing – original draft, Investigation, Formal analysis, Data curation. **Maria Rohm:** Writing – review & editing, Writing – original draft, Investigation, Formal analysis, Data curation. **Lykke Sylow:** Writing – review & editing, Writing – original draft, Supervision, Resources, Project administration, Methodology, Investigation, Funding acquisition, Formal analysis, Data curation, Conceptualization. **Steffen H. Raun:** Writing – review & editing, Writing – original draft, Visualization, Validation, Supervision, Resources, Project administration, Methodology, Investigation, Funding acquisition, Formal analysis, Data curation, Conceptualization.

DECLARATION OF GENERATIVE AI AND AI-ASSISTED TECHNOLOGIES IN THE WRITING PROCESS

Statement: During the preparation of this work, the authors used ChatGPT to do minor corrections and shorten sentences. After using this tool/service, the authors reviewed and edited the content as needed and we take full responsibility for the content of the published article.

FUNDING

SHR was funded by Independent Research Fund Denmark (2030-00007A), the Lundbeck Foundation (R380-2021-1451) and the Novo Nordisk Foundation (NNF0101703). TCPP was funded by the Lundbeck Foundation (R449-2023-1468) and the Novo Nordisk Foundation (NNF24OC0088823). JRK was funded by Novo Nordisk Foundation (17SA0031406) and Independent Research Fund Denmark (9058-00047B). MR was funded by the European Research Council (ERC) under the European Union's Horizon 2020 research and innovation program (STOPWASTE no. 949017), an EFSD/Novo Nordisk Foundation Future Leaders Award, the German Centers for Health Research (DZG) innovation fund and by the German Research Foundation (DFG FOR5795-1_HyperMet).

DECLARATION OF COMPETING INTEREST

The authors declare that they have no known competing financial interests or personal relationships that could have appeared to influence the work reported in this paper.

ACKNOWLEDGEMENT

We thank our colleagues at the Molecular Metabolism in Cancer and Aging Group, Faculty of Health and Medical Sciences, University of Copenhagen, for profitable discussions on this topic. We acknowledge the Rodent Metabolic Phenotyping Platform (RMPP), Novo Nordisk Foundation Center for Metabolic Research, University of Copenhagen, for the use of their facilities. We also acknowledge Simon Bech Petersen, Department of Biomedical Sciences, Faculty of Health and Medical Sciences, University of Copenhagen, and Raul Terron Exposito, Institute for Diabetes and Cancer, Helmholtz Munich, for their assistance. Illustrations were generated using Biorender.com (RRID:SCR_018361) and ©Inkscape. Graphs were generated with GraphPad PRISM (RRID:SCR_002798).

REFERENCES

[1] Fearon K, Strasser F, Anker SD, Bosaeus I, Bruera E, Fainsinger RL, et al. Defi nition and classifi cation of cancer cachexia: an international consensus. Www Thelancet Com/Oncology 2011;12:489–95. https://doi.org/10.1016/S1470.

[2] Baracos VE, Martin L, Korc M, Guttridge DC, Fearon KCH. Cancer-associated cachexia. Nat Rev Dis Primers 2018. https://doi.org/10.1038/nrdp.2017.105.

[3] Dev R, Bruera E, Dalal S. Insulin resistance and body composition in cancer patients. Ann Oncol 2018;29:ii18–26. https://doi.org/10.1093/annonc/mdx815.

[4] Màrmol JM, Carlsson M, Raun SH, Grand MK, Sørensen J, Lang Lehrskov L, et al. Insulin resistance in patients with cancer: a systematic review and meta-analysis. Acta Oncol 2023;62(4):364–71. https://doi.org/10.1080/0284186X.2023.2197124.

[5] Tayek JA. A review of cancer cachexia and abnormal glucose metabolism in humans with cancer. J Am Coll Nutr 1992;11(4):445–56. https://doi.org/10.1080/07315724.1992.10718249.

[6] Chiefari E, Mirabelli M, La Vignera S, Tanyolaç S, Foti DP, Aversa A, et al. Insulin resistance and cancer: in search for a causal link. Int J Mol Sci 2021. https://doi.org/10.3390/ijms222011137.

[7] Tam CS, Xie W, Johnson WD, Cefalu WT, Redman LM, Ravussin E. Defining insulin resistance from hyperinsulinemic-euglycemic clamps. Diabetes Care 2012;35(7):1605–10. https://doi.org/10.2337/DC11-2339.

[8] Sylow L, Grand MK, von Heymann A, Persson F, Siersma V, Kriegbaum M, et al. Incidence of new-onset type 2 diabetes after cancer: a Danish cohort study. Diabetes Care 2022;45(6):e105–6. https://doi.org/10.2337/DC22-0232.

[9] Hwangbo Y, Kang D, Kang M, Kim S, Lee EK, Kim YA, et al. Incidence of diabetes after cancer development: a Korean national cohort study. JAMA Oncol 2018;4(8):1099. https://doi.org/10.1001/JAMAONCOL.2018.1684.

[10] Han X, Raun SH, Carlsson M, Sjøberg KA, Henriquez-Olguín C, Ali M, et al. Cancer causes metabolic perturbations associated with reduced insulin-stimulated glucose uptake in peripheral tissues and impaired muscle microvascular perfusion. Metab Clin Exp 2020;105. https://doi.org/10.1016/j.metabol.2020.154169.

[11] Raun SH, Knudsen JR, Han X, Jensen TE, Sylow L. Cancer causes dysfunctional insulin signaling and glucose transport in a muscle-type-specific manner. FASEB (Fed Am Soc Exp Biol) J 2022;36(3). https://doi.org/10.1096/fj.202101759R.

[12] Counts BR, Halle JL, Carson JA. Early onset physical inactivity and metabolic dysfunction in tumor-bearing mice is associated with accelerated cachexia. Med Sci Sports Exerc 2022;54(1):77. https://doi.org/10.1249/MSS.0000000000002772.

[13] Asp ML, Tian M, Kliewer KL, Belury MA. Rosiglitazone delayed weight loss and anorexia while attenuating adipose depletion in mice with cancer cachexia. Cancer Biol Ther 2011;12(11):957–65. https://doi.org/10.4161/cbt.12.11.18134.

[14] Asp ML, Tian M, Wendel AA, Belury MA. Evidence for the contribution of insulin resistance to the development of cachexia in tumor-bearing mice. Int J Cancer 2010;126(3):756–63. https://doi.org/10.1002/ijc.24784.

[15] Chovsepian A, Prokopchuk O, Petrova G, Gjini T, Kuzi H, Heisz S, et al. Diabetes increases mortality in patients with pancreatic and colorectal cancer by promoting cachexia and its associated inflammatory status. Mol Metabol 2023;73. https://doi.org/10.1016/j.molmet.2023.101729.

[16] Raun SH, Ali MS, Han X, Henríquez-Olguín C, Pham TCP, Meneses-Valdés R, et al. Adenosine monophosphate-activated protein kinase is elevated in human cachectic muscle and prevents cancer-induced metabolic dysfunction in mice. J Cachexia Sarcopenia Muscle 2023;14(4):1631–47. https://doi.org/10.1002/jcsm.13238.

[17] Sørensen J, Hammershøi A, Màrmol JM, Lehrskov LL, Nørgaard O, Sylow L. Revisiting insulin resistance in human cancer cachexia — a systematic review and meta-analysis. 2025. https://doi.org/10.1101/2025.03.28.25324822.

[18] Morigny P, Vondrackova M, Ji H, Brejchova K, Krakovkova M, Makris K, et al. Multi-omics profiling of cachexia-targeted tissues reveals a spatio-temporally coordinated response to cancer. Nat Metab 2026. https://doi.org/10.1038/s42255-025-01434-3.

[19] Yeom E, Yu K. Understanding the molecular basis of anorexia and tissue wasting in cancer cachexia. Exp Mol Med 2022:426–32. https://doi.org/10.1038/s12276-022-00752-w.

[20] Ezeoke CC, Morley JE. Pathophysiology of anorexia in the cancer cachexia syndrome. J Cachexia Sarcopenia Muscle 2015:287–302. https://doi.org/10.1002/jcsm.12059.

[21] Amitani M, Asakawa A, Amitani H, Inui A. Control of food intake and muscle wasting in cachexia. Int J Biochem Cell Biol 2013:2179–85. https://doi.org/10.1016/j.biocel.2013.07.016.

[22] Fu J, Liu S, Li M, Guo F, Wu X, Hu J, et al. Optimal fasting duration for mice as assessed by metabolic status. Sci Rep 2024;14(1). https://doi.org/10.1038/s41598-024-72695-3.

[23] Anson RM, Guo Z, De Cabo R, Iyun T, Rios M, Hagepanos A, et al. Intermittent fasting dissociates beneficial effects of dietary restriction on glucose metabolism and neuronal resistance to injury from calorie intake. Proc Natl Acad Sci 2003;100(10). https://doi.org/10.1073/pnas.1035720100.

[24] Kalant N, Stewart J, Kaplan R. Effect of diet restriction on glucose metabolism and insulin responsiveness in aging rats. Mech Ageing Dev 1988;46(1–3):89–104. https://doi.org/10.1016/0047-6374(88)90117-0.

[25] Raun SH, Henriquez-Olguín C, Karavaeva I, Ali M, Møller LLV, Kot W, et al. Housing temperature influences exercise training adaptations in mice. Nat Commun 2020;11(1):1560. https://doi.org/10.1038/s41467-020-15311-y.

[26] Welinder C, Ekblad L. Coomassie staining as loading control in Western blot analysis. J Proteome Res 2011;10(3):1416–9. https://doi.org/10.1021/pr1011476.

[27] Raun SH, Braun JL, Karavaeva I, Henriquez-Olguín C, Ali MS, Møller LLV, et al. Mild cold stress at ambient temperature elevates muscle calcium cycling and exercise adaptations in obese female mice. Endocrinology 2024;165(10). https://doi.org/10.1210/endocr/bqae102.

[28] Irazoki A, Frank E, Cam Phung Pham T, Braun JL, Ehrlich AM, Haid M, et al. Journal of cachexia, sarcopenia and muscle housing temperature impacts the systemic and tissue-specific molecular responses to cancer in mice. J Cachexia Sarcopenia Muscle 2025;16:13781. https://doi.org/10.1002/jcsm.13781.

[29] Pasquale V, Dugnani E, Liberati D, Marra P, Citro A, Canu T, et al. Glucose metabolism during tumorigenesis in the genetic mouse model of pancreatic cancer. Acta Diabetol 2019;56(9):1013–22. https://doi.org/10.1007/s00592-019-01335-4.

[30] Sylow L, Tokarz VL, Richter EA, Klip A. The many actions of insulin in skeletal muscle, the paramount tissue determining glycemia. Cell Metab 2021:758–80. https://doi.org/10.1016/j.cmet.2021.03.020.

[31] Sancak Y, Thoreen CC, Peterson TR, Lindquist RA, Kang SA, Spooner E, et al. PRAS40 is an insulin-regulated inhibitor of the mTORC1 protein kinase. Mol Cell 2007;25(6):903–15. https://doi.org/10.1016/j.molcel.2007.03.003.

[32] Haar E Vander, Lee S, Bandhakavi S, Griffin TJ, Kim D-H. Insulin signalling to mTOR mediated by the Akt/PKB substrate PRAS40. Nat Cell Biol 2007;9(3):316–23. https://doi.org/10.1038/ncb1547.

[33] Morigny P, Ji H, Cussonneau L, Zorzato S, Kwon Y, Riols F, et al. Inhibition of ceramide synthesis ameliorates body wasting in a cancer cachexia model. J Clin Investig 2026;136(10). https://doi.org/10.1172/JCI194687.

[34] Huang S, Czech MP. The GLUT4 glucose transporter. Cell Metab 2007;5(4):237–52. https://doi.org/10.1016/j.cmet.2007.03.006.

[35] Silvestre MFP, Viollet B, Caton PW, Leclerc J, Sakakibara I, Foretz M, et al. The AMPK-SIRT signaling network regulates glucose tolerance under calorie restriction conditions. Life Sci 2014;100(1):55–60. https://doi.org/10.1016/j.lfs.2014.01.080.

[36] Sequea DA, Sharma N, Arias EB, Cartee GD. Calorie restriction enhances insulin-stimulated glucose uptake and akt phosphorylation in both fast-twitch and slow-twitch skeletal muscle of 24-month-old rats. Journals of Gerontology - Series A Biological Sciences and Medical Sciences 2012;67(12):1279–85. https://doi.org/10.1093/gerona/gls085.

[37] Gazdag AC, Dumke CL, Kahn CR, Cartee GD. Calorie restriction increases insulin-stimulated glucose transport in skeletal muscle from IRS-1 knockout mice, vol. 48; 1930.

[38] Delfinis LJ, Bellissimo CA, Gandhi S, DiBenedetto SN, Garibotti MC, Thuhan AK, et al. Muscle weakness precedes atrophy during cancer cachexia and is linked to muscle-specific mitochondrial stress. JCI Insight 2022;7(24). https://doi.org/10.1172/jci.insight.155147.

[39] Berriel Diaz M, Rohm M, Herzig S. Cancer cachexia: multilevel metabolic dysfunction. Nat Metab 2024;6(12):2222–45. https://doi.org/10.1038/s42255-024-01167-9.

[40] Tisdale MJ. Biology of cachexia. JNCI Journal of the National Cancer Institute 1997;89(23):1763–73. https://doi.org/10.1093/jnci/89.23.1763.

